The S5/S6 STAMP all-sky search for long-duration gravitational-wave transients

Tanner Prestegard for the STAMP all-sky working group

University of Minnesota

November 2, 2015

LIGO-P1400138

Pipeline overview

- Looking for long-duration unmodeled GW transients ($\approx 10 - 500$ s).
  - Accretion disk instabilities and fragmentation.
  - Rotational instabilities in PNS remnants, PNS convection, r-modes, and more.
- Procedure:
  - Cross-correlate data from multiple IFOs.
  - Make *ft*-maps of cross- and auto-power.
  - Apply clustering algorithm to pick out significant clusters.

STAMP all-sky working group:
Marie Anne Bizouard, Nelson Christensen, Michael Coughlin, Samuel Franco (graduated), Valentin Frey, Patrice Hello, Vuk Mandic, Tanner Prestegard, and Eric Thrane.

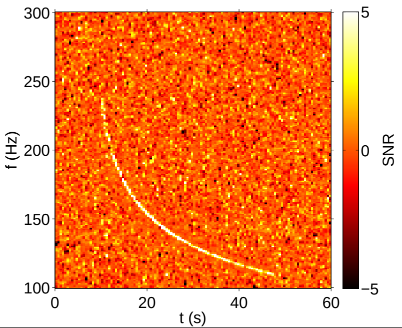

Figure 1: STAMP SNR *ft*-map, including a simulated GW signal. This is an energy SNR.

Search description

Data selection:

- S5: 283.0 days of coincident H1-L1 data.
- S6: 132.9 days of coincident H1-L1 data.
- CAT 1 flags: from stochastic isotropic search, added burst injection flags.
- 100 time-slides from each science run.
- Data divided into 500 second-long *ft*-maps, 50% overlapping.
- Frequency range: 40 - 1000 Hz.

Data quality:

- STAMP glitch cut: checks for consistency between detectors using auto-power spectra[1].
- Frequency notches: primarily 60 Hz harmonics, violin modes, calibration lines.

[1] T. Prestegard et al., Class. Quantum Grav. **29**, 095018 (2012).

Background study results

Post-processing cuts:

- SNRfrac: veto triggers that deposit more than 45% of their power in a single time segment. Threshold tuned to maximize search sensitivity.
- CAT 2 DQ flags: chosen by estimating significance of coincidence with 100 loudest triggers from background studies. Used only for GW candidate follow up.

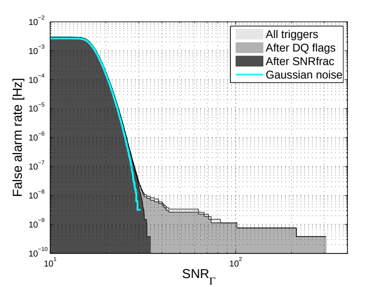

(a) S5, 100 time-slides.

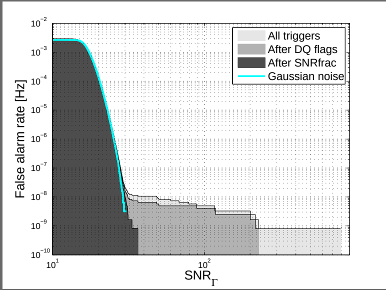

(b) S6, 100 time-slides.

Injection studies

All waveforms range between 9 - 250 s in duration and 50 - 900 Hz.

Waveforms:

- Four accretion disc instability (ADI) waveforms[2,3].
- Two monochromatic waveforms.
- Two linear (frequency-time evolution) waveforms.
- Two quadratic (frequency-time evolution) waveforms.
- Two sine-Gaussian waveforms.
- Three band-limited white noise burst waveforms.

Details:

- Waveforms injected at 1500 random times in each dataset.
- Each waveform studied at 16 different signal amplitudes.
- Total: 1500 trials per waveform per amplitude per dataset.
- Random sky position and waveform polarization.

[2] M. H. van Putten et al., Phys. Rev. D **69**, 044007 (2004).
[3] C. D. Ott and L. Santamaría, LIGO DCC T1100093 (2011).

Waveform plots

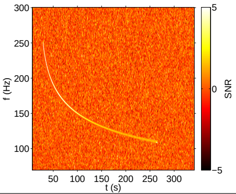

(a) ADI-C.

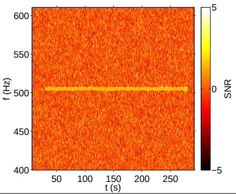

(b) MONO-B.

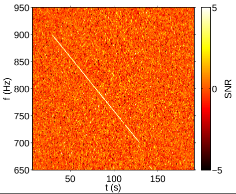

(c) LINE-B.

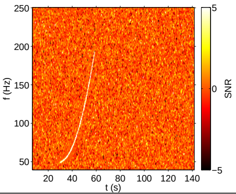

(d) QUAD-A.

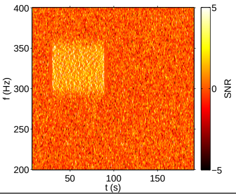

(e) WNB-B.

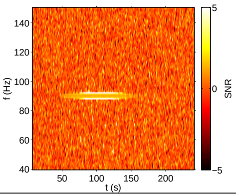

(f) SG-A.

Zero-lag results

Loudest triggers:

Dataset	SNR_Γ	FAR [yr^{-1}]	FAP	GPS time	Freq. [Hz]
S5	29.65	1.00	0.54	851136555.0	129 - 201
S6	27.13	6.94	0.92	958158359.5	537 - 645

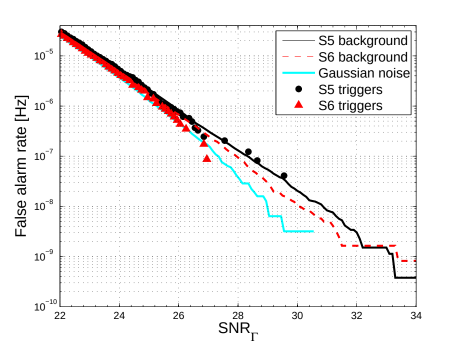

Figure 2: S5 and S6 zero-lag triggers superimposed on time-slide triggers.

Upper limits

Loudest event statistic (visible volume):

$$R_{90\%,\mathrm{VT}} = \frac{2.3}{\sum_k V_{\mathrm{vis},k}(\mathrm{FAD}^\star) \times T_{\mathrm{obs},k}}$$

Waveform	V_{vis} [Mpc^3] S5	V_{vis} [Mpc^3] S6	$R_{90\%,\mathrm{VT}}$ [Mpc^{-3}yr^{-1}]
ADI-A	1.6×10^3	3.2×10^3	1.0×10^{-3}
ADI-B	5.4×10^4	8.6×10^4	3.6×10^{-5}
ADI-C	7.0×10^3	1.4×10^4	2.4×10^{-4}
ADI-E	1.5×10^4	2.9×10^4	1.1×10^{-4}

Table 1: Visible volume upper limits on ADI waveforms. Uncertainties included; they are dominated by calibration error and marginalized over using a Bayesian method.

Loudest event statistic (efficiency):

$$R_{90\%,\mathrm{T}} = \frac{2.3}{\sum_k \epsilon_k(\mathrm{SNR}^\star_{\Gamma,k})\, T_{\mathrm{obs},k}}$$

Plots on next slide.

Upper limits - efficiency

Rate upper limit vs. h_{rss} curves for all waveforms considered in the injection study.

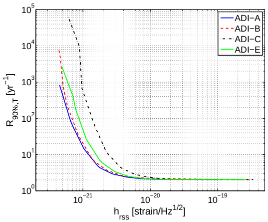

(a) ADI waveforms.

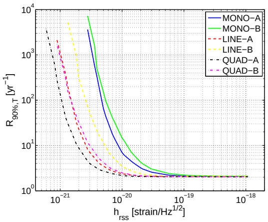

(b) Sinusoidal waveforms.

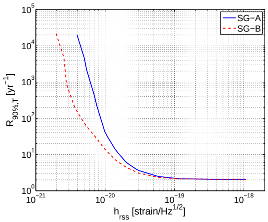

(c) Sine-Gaussian waveforms.

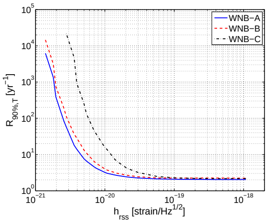

(d) White noise burst waveforms.

Conclusions

Difficult to compare results directly to short-transient searches due to usage of different waveforms. Longer waveforms will require a more energetic source since the energy is more dispersed in time. Estimates of isotropic energy are still $\approx 2-4$ orders of magnitude above the literature[4].

First all-sky upper limits on long-lasting GW transients with LIGO data.

Review has been completed (see talk from reviewers).

Search is now focusing on O1 data.

Paper draft on the DCC, comments welcome! LIGO-P1400138

Target journal: PRD.

[4] E. Mueller et al., Astrophys. J **603**, 221 (2004).

Extra Slides

Analysis description

1. Calculate cross-power and auto-power *ft*-maps.
2. Notch problematic frequency bins.
3. Check each *ft*-map column with the STAMP glitch flag[5] and notch columns identified as glitchy.
4. Run clustering algorithm on SNR *ft*-map.
5. If a cluster was found, calculate cluster statistics.
6. Save results for post-processing.

[5] T. Prestegard et al., Class. Quantum Grav. **29**, 095018 (2012).

Clustering overview

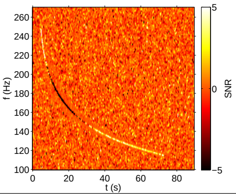

(a) SNR *ft*-map.

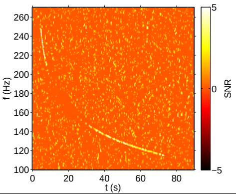

(b) Apply positive threshold.

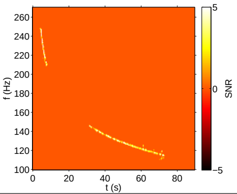

(c) Find positive clusters.

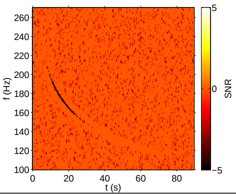

(d) Apply negative threshold.

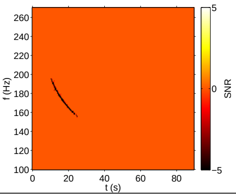

(e) Find negative clusters.

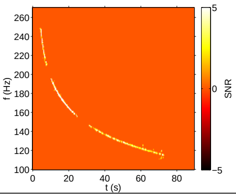

(f) Form larger clusters, apply absolute value, calculate cluster statistics.

ADI waveform details

Waveform	$M[M_\odot]$	a^*	ϵ	Duration [s]	Frequency [Hz]
ADI-A	5	0.30	0.050	39	135 - 166
ADI-B	10	0.95	0.200	9	110 - 209
ADI-C	10	0.95	0.040	236	130 - 251
ADI-E	8	0.99	0.065	76	111 - 234

Table 2: List of ADI waveforms used to test the sensitivity of the search. Here, M is the mass of the central black hole, a^* is the dimensionless Kerr spin parameter of central black hole, and ϵ is the fraction of the disk mass that forms clumps. Frequency refers to the ending and starting frequencies of the GW signal, respectively. All waveforms have an accretion disk mass of 1.5 $M_\odot$.

Sinusoidal waveform details

Waveform	Duration [s]	f_0 [Hz]	$\frac{df}{dt}$ [Hz/s]	$\frac{d^2f}{dt^2}$ [Hz/s^2]
MONO-A	150	90	0.0	0.00
MONO-B	250	505	0.0	0.00
LINE-A	250	50	0.6	0.00
LINE-B	100	900	-2.0	0.00
QUAD-A	30	50	0.0	0.33
QUAD-B	70	500	0.0	0.04

Table 3: List of sinusoidal waveforms used to test the sensitivity of the search. Here, f_0 is the initial frequency of the signal, $\frac{df}{dt}$ is the frequency derivative, and $\frac{d^2f}{dt^2}$ is the second derivative of the frequency.

WNB and SG waveform details

Waveform	Duration [s]	f_0 [Hz]	τ [s]
SG-A	150	90	30
SG-B	250	505	50

Table 4: List of sine-Gaussian waveforms used to test the sensitivity of the search. Here, τ is the decay time of the Gaussian envelope.

Waveform	Duration [s]	Frequency band [Hz]
WNB-A	20	50 - 400
WNB-B	60	300 - 350
WNB-C	100	700 - 750

Table 5: List of band-limited white noise burst waveforms used to test the sensitivity of the search.

Injection study results

Efficiency vs. h_{rss} curves for all waveforms considered in the injection study. Curves shown are for S6 and include SNRfrac vetoes and CAT 2 data quality flags.

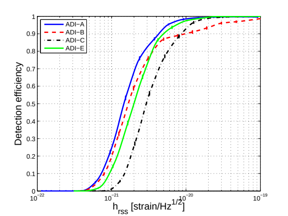

(a) ADI waveforms.

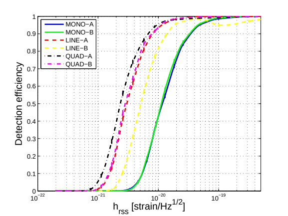

(b) Sinusoidal waveforms.

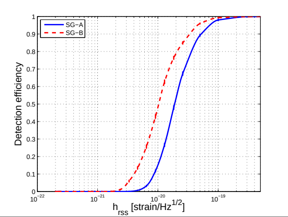

(c) Sine-Gaussian waveforms.

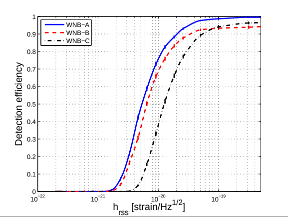

(d) White noise burst waveforms.

Energy calculations

Difficult to compare results directly to short-transient searches due to usage of different waveforms. Longer waveforms will require a more energetic source since the energy is more dispersed in time.

Can estimate isotropic energy for a pair of rotating point masses:

$E_{\mathrm{GW}} \simeq h^2_{\mathrm{rss},50\%} r^2_{50\%} \pi^2 f^2_{\mathrm{GW}} \frac{c^3}{G}$.

For *ad hoc* waveforms, we fix a fiducial distance of 10 kpc.

Results:

- ADI: $1.3 \times 10^{-7} - 1.2 \times 10^{-6}\ \mathrm{M_\odot c^2}$.
- Sinusoidal: $6.1 \times 10^{-7} - 2.3 \times 10^{-4}\ \mathrm{M_\odot c^2}$.
- Sine-Gaussian: $1.1 \times 10^{-5} - 2.5 \times 10^{-4}\ \mathrm{M_\odot c^2}$.
- White noise bursts: $2.1 \times 10^{-5} - 5.4 \times 10^{-4}\ \mathrm{M_\odot c^2}$.

Compare to a protoneutron star at 10 kpc developing matter convection over 30 s: $4 \times 10^{-9}\ \mathrm{M_\odot c^2}$.[6]

[6] E. Mueller et al., Astrophys. J **603**, 221 (2004).